

Ruei-Zeng Lin · Li-Fang Chou ·  
Chi-Chen Michael Chien · Hwan-You Chang

## Dynamic analysis of hepatoma spheroid formation: roles of E-cadherin and $\beta$ 1-integrin

Received: 5 June 2005 / Accepted: 12 December 2005 / Published online: 18 February 2006  
© Springer-Verlag 2006

**Abstract** A spheroid is an in vitro multicellular aggregate that provides a microenvironment resembling that of normal tissue in vivo. Although cell adhesion molecules such as integrins and cadherins have been implicated in participating in the process of spheroid formation, little is known about the timing of their action. In this study, we have employed an image-based quantitative method to investigate the compactness of cell aggregates during hepatoma spheroid formation in a dynamic fashion. By modulating  $\beta$ 1-integrin and E-cadherin activity with specific blocking antibodies, ion chelators, and RGD-sequence-containing peptides, we show that these cell adhesion molecules mediate the formation of spheroids through the establishment of complex cell-cell and cell-extracellular matrix (ECM) interactions. The dynamics of spheroid formation can be separated into three stages. In the first stage, ECM fibers act as a long-chain linker for the attachment of dispersed single-cells to form loose aggregations through the binding of integrins. This is followed by a delay period in which cell aggregates pause in compaction, presumably because of the accumulation of sufficient amounts of E-cadherins. In the third stage, strong homophilic interaction of E-cadherins is a major factor for the morphological transition from loose cell aggregates to

compact spheroids. These findings thus provide comprehensive information on the molecular mechanisms and dynamics of hepatoma spheroid formation.

**Keywords** Aggregates · Cadherins · Dynamics · Integrins · Spheroids · Hepatoma cell lines (Human)

### Introduction

Since the pioneer studies of Holtfreter (1944) and the Mosconas (Moscona and Moscona 1952), which introduced re-assembly of cultured embryonic and malignant cells into spheroids, the three-dimensional cell culture technique has been exploited widely in many topics of biomedical research. In comparison with conventional monolayer cultures, which are unable to generate the normal cell-cell interaction found in vivo, cells in spheroids more closely resemble the situation in vivo with regard to differentiation patterns and to spatial cell-cell and cell-extracellular matrix (ECM) interactions (Kunz-Schughart et al. 1998; Mueller-Klieser 1997). Because of these advantages, spheroids are being increasingly used as a model in research fields such as cancer treatment, apoptosis, differentiation, and tissue morphogenesis (Bates et al. 2000; Desoize 2000). In addition, the use of functional organoid tissues generated by spheroid techniques also contributes to the advance in tissue engineering, stem cell research, and regenerative medicine (Jakab et al. 2004; Kale et al. 2000).

As in embryonic development and tissue morphogenesis, complex cell adhesion and differentiation contribute to the formation of multicellular spheroids. Several reports have described the roles of cadherins and integrins in the spheroid-forming process (Casey et al. 2001; Robinson et al. 2003, 2004; Shimazui et al. 2004). Cadherins are a large family of  $\text{Ca}^{2+}$ -dependent transmembrane proteins that bind to each other by homophilic interactions (Angst et al. 2001). The classical cadherin, viz., E-cadherin, is the best-studied member of the family and the most abundantly expressed type in epithelial tissues (Marrs et al. 1995). E-

This work was supported by the National Program of Genome Medicine, ROC (NSC 93-3112-B007-001) and Veteran General Hospitals University System of Taiwan Joint Research Program (VGHUST94-G6-06-3).

R.-Z. Lin · L.-F. Chou · H.-Y. Chang (✉)  
Institute of Molecular Medicine,  
National Tsing Hua University,  
101 Kuang Fu Road, 2nd Sec.,  
Hsin Chu 300, Taiwan, Republic of China  
e-mail: hychang@life.nthu.edu.tw  
Tel.: +886-3-5742910  
Fax: +886-3-5742910

C.-C. M. Chien  
Department of Obstetrics and Gynecology,  
Ton-Yen General Hospital,  
69 Sian Jheng Sec. Road,  
Chubei 302, Taiwan, Republic of China

cadherin has been demonstrated to generate strong cell cohesion and is known as a mediator of spheroid formation in several cell types, including primary hepatocytes (Nakamura et al. 2002) and cells of renal carcinoma (Shimazui et al. 2004), breast cancer (Alpaugh et al. 2002; Tomlinson et al. 2001), and prostate cancer (Enmon et al. 2002). Integrins are also a large family of proteins that function as heterodimers of  $\alpha$ - and  $\beta$ -subunits and act to link cells to ECM proteins (Guo and Giancotti 2004). Interactions of integrin and ECMs are generally regarded as critical for the promotion of cell migration and invasion, which is the opposite of the role of E-cadherin in the maintenance of tissue integrity. Nevertheless, at least in the case of  $\alpha 5 \beta 1$ -integrin and fibronectin, integrin-ECM-mediated cell contact has been shown to regulate the formation of spheroids of several cell types (Casey et al. 2001; Robinson et al. 2003, 2004). The stage of spheroid formation at which these molecules actually work however remains obscure.

Many types of cell can self-aggregate into spheroids in non-adherent containers or continuous stirring spinner flasks. Alternatively, cells can be put under a microgravity conditions in hanging drops to promote spheroid formation (Kelm et al. 2003). This method is laborious but provides the best control of spheroid size because a specific number of suspended cells can be assembled to form a single spheroid. The compactness and cohesive force between cells of such a spheroid can be measured by techniques including tissue surface tensiometry (Robinson et al. 2004) and the flow-chamber-based cell detachment assay (Byers et al. 1995). These methods in general might provide accurate measurements of the force of cell-cell interaction but are either destructive or unable to reveal the detail changes in compactness that occur during spheroid assembly. On the other hand, several studies have addressed the kinetics of spheroid aggregation through image analysis and mathematic modeling (Enmon et al. 2001, 2002; Neelamegham et al. 1997). However, few correlations between the proposed model and possible molecular mechanisms have been made.

In this paper, we describe the results of our attempts to dissect the process of single hepatoma cell assemble into compact spheroids. By analyzing spheroid formation in a time-lapse fashion, we have been able to discern that the process takes place in three stages: an initial rapid aggregation, followed by a delay period, and further tight compaction. The cell adhesion molecules participating in each of the stages have also been examined.

---

## Materials and methods

### Cell lines and growth conditions

Human hepatoma cell lines HepG2/C3A (ATCC HB8065), PLC/PRF/5 (ATCC CRL-8024), and Hep3B (ATCC HB8064) were maintained at 37°C in 95% air/5% CO<sub>2</sub> in Iscove's modified Dulbecco's medium (IMDM; Gibco-

BRL, N.Y.) containing 10% (v/v) heat-inactivated fetal bovine serum (FBS; Biological Industries, Israel) and antibiotics (100 U/ml penicillin and 100 U/ml streptomycin; Sigma-Aldrich, Mo.) unless otherwise indicated. The lymphatic cell line Ramos (ATCC CRL-1596) was maintained similarly, except that RPMI-1640 medium (Gibco-BRL) was used.

### Generation of spheroids

The hanging drop technique used for cultivating embryoid bodies of embryonic stem cells was employed to generate hepatoma spheroids of defined sizes and cell numbers (Kelm et al. 2003). Cells detached from near-confluent dishes were re-suspended in IMDM containing 2% FBS, and the number of cells was counted by using a hemacytometer. Approximately 50 drops of cell suspension, each 20  $\mu$ l in size and containing approximately 500 cells, were deposited onto the underside of the lid of a 10-cm tissue culture dish. Each lid was coated with a thin layer of poly-dimethylsiloxane (PDMS), which provided a strong hydrophobic surface to enhance the coherence of the water drops and thereby to maintain their shape while being handled. The culture dishes upon which the lids were placed were filled with 8 ml phosphate balanced saline (PBS) to prevent the hanging drops vaporizing. The microgravity conditions in each hanging drop concentrated the cells, which then formed a single spheroid at the liquid-air interface.

### Quantification of spheroid compactness

The progression of spheroid formation within hanging drops was quantitatively analyzed by the area coverage method (Robinson et al. 2004) with modifications. A digital camera attached to an upright microscope was used to capture high contrast images of the cells in the hanging drops directly through the culture lids. A series of time-lapse images following the spheroid-forming process were recorded every 2 h. The total area occupied by cells within an image was determined by circumscribing the perimeters, marking the entire area, and calculating the pixel numbers by using image processing software (PhotoImpact 6, Ulead Systems, Taiwan). The projected area of the spheroid was further converted into its approximate three-dimensional volume by taking the square root of the area to the third power. For each time point, cell aggregates from 60 hanging drops were measured from three individual experiments to obtain the mean volume ( $\pm$ SD). Finally, all the data were divided by that of the same group at the first 2-h time point to normalize the variation that may have resulted from the difference in initial cell number. This yielded the Compactness Index (CI). A small CI value indicated the greater degree of compactness of the cell aggregates. Alternatively, the changes of shrinkage rate ( $\Delta$ CI/ $\Delta$ t), which could be calculated from the difference in spheroid volumes between two specific time points, was

also used to provide a sensitive measurement of the progression of spheroid formation.

#### Reverse transcription and real-time polymerase chain reaction

Total RNA was isolated by using the TRI Reagent (Molecular Research Center, Ohio), and the residual genomic DNA was removed by treatment with RNase-free DNase. Total RNA (2 µg) was reverse-transcribed in a 20-µl reaction mixture containing 50 U Moloney murine leukemia virus reverse transcriptase, 5 µM dithiothreitol (both from Invitrogen, Calif.), 40 U RNaseOUT Recombinant Ribonuclease Inhibitor (Promega, Calif.), 0.5 µM oligo-dT primer, 0.5 µM random hexanucleotide primers (both from Amersham Pharmacia Biotech, N.J.), and 500 µM deoxynucleoside triphosphate mixture (dNTPs mix). Reverse transcription was carried out at 50°C for 60 min. The reaction was subsequently terminated by heating the mixture at 70°C for 15 min, and the cDNA was stored at -20°C.

All real-time polymerase chain reaction (PCR) analyses were performed on an ABI PRIZM 7000 instrument with the primers detailed in Table 1. Each reaction included a 25-µl reaction mixture containing 0.1 µM each primer, 12.5 µl 2× SYBR Green PCR Master Mix (Applied Biosystem, including AmpliTaq Gold DNA polymerase with buffer, dNTPs mix, SYBR Green I dye, Rox dye, and 10 mM MgCl<sub>2</sub>), and 1 µl template cDNA. A typical amplification program included activation of the enzyme at 94°C for 10 min, followed by 40 cycles of denaturation at 94°C for 15 s, and annealing and extension at 60°C for 1 min. Minor modifications were made on the standard amplification program for certain sets of primer to eliminate the production of non-specific products. The C<sub>T</sub> (threshold of cycle) value for each gene was determined by the automated threshold analysis function of the ABI instrument and normalized to C<sub>T(β-actin)</sub> to obtain dC<sub>T</sub> (=C<sub>T(β-actin)</sub>-C<sub>T(test)</sub>). The difference in E-cadherin expres-

sion at different time points were indicated by the ddC<sub>T</sub> values, which were calculated as dC<sub>T(indicated-h)</sub>-dC<sub>T(0-h)</sub>. The difference of *n* between two C<sub>T</sub> values (dC<sub>T</sub>) indicated a 2<sup>*n*</sup>-fold difference in the amount of the target sequence between the two cDNA samples being compared.

#### Quantification of ECM proteins secreted from cells

The amount of ECM proteins secreted from different hepatoma cells was evaluated by the functional cell adhesion assay. In brief, conditioned medium was collected from near-confluent monolayer dishes or pooled from approximately 500 hanging drops, each with a spheroid containing approximately 500 cells, which had been cultured in IMDM with 2% FBS for 12 h. Cells and debris were removed from the conditioned medium by centrifugation. Non-adhesive 96-well ELISA plates (Nunc, Denmark) were incubated with the conditioned medium for 12 h at 37°C and washed twice with PBS. Approximately 5×10<sup>4</sup> HepG2 cells grown in IMDM with 2% FBS were labeled with green fluorescent membrane binding dye DiO (Molecular Probes, Ore.), added to each well, and incubated for 4 h at 37°C. The floating cells were gently rinsed off with PBS, and the quantity of attached cells was determined by measuring light emission in a Wallac 1420 VICTOR2 fluorescence plate reader (Perkin Elmer, Mass.).

#### Determination of permeability of spheroids to small molecules

Approximately 30 cell aggregates were collected from the hanging drops and transferred into a test tube by using a micropipette with head-cut tips. The cell-membrane-binding dye 1,1'-dioctadecyl 3,3',3',3'-tetramethylindocarbocyanine perchlorate (DiI; Molecular Probes) was added to the hanging drop cultures at a final concentration of 5 µM at various time points and was allowed to diffuse freely for 15 min at 25°C. The labeled cell aggregates were

**Table 1** Properties and sequences of PCR primers used

Target gene	Primer position	Sequence 5'→3'	Amplicon size (bp)
E-cadherin	Forward	TGCCCGAGAAAATGAAAAAGG	199
	Reverse	GTGTATGTGGCAATGCGTTC	
N-cadherin	Forward	CCATCACTCGGCTTAATGGT	194
	Reverse	ACCCACAATCCTGTCCACAT	
P-cadherin	Forward	GGAACCCTTCTGCTAACACT	218
	Reverse	CAAGACCACTGTGTCACCTT	
VE-cadherin	Forward	CAGCCCAAAGTGTGTGAGAA	185
	Reverse	CGGTCAAACCTGCCATACTT	
LI-cadherin	Forward	GACAATCGACCCACGTTCT	203
	Reverse	GCTCCCGTTTTGTTGTTGAT	
β1-Integrin	Forward	CATCTGCGAGTGTGGTGTCT	209
	Reverse	GGGGTAATTTGTCCCGACTT	
β-Actin	Forward	CATGGAGTCCTGGCATCCACGAACT	148
	Reverse	ATCTCCTTCTGCATCCTGTCCGCATA	

allowed to sediment, and the supernatant was removed by gentle suction. After being rinsed briefly with PBS, the cell aggregates were fixed for 15 min in PBS containing 2% formaldehyde and 0.05% glutaraldehyde, washed with PBS, and then counter-stained with the nucleus-labeling dye Hoechst 33342. A confocal microscope (LSM 510, Zeiss, Germany) was used to obtain optical sections near the center of the stained aggregates to assess the permeability of DiI. The HepG2 spheroids that were completely stained with the same dye by prolonged incubation were used as a positive control.

#### Effects of ECM, integrin, and E-cadherin activities on spheroid formation

Single-cell suspensions of HepG2 and PLC/PRF/5 cells were tested in the hanging drop assays in the presence of various concentrations of rat type I collagen (Vitrogen, N. J.), fibronectin, or gelatin (Sigma-Aldrich). To modulate integrin activity, 1 mM MgCl<sub>2</sub>, 10 µg/ml β1-integrin-specific monoclonal antibody (mAb) clone P4G11 and P5D2 (Santa Cruz Biotechnology, Calif.), 10 µg/ml blocking RGD peptide, and the control RAD peptide (Calbiochem, Calif.) were added, respectively, into the hanging drops (Casey et al. 2001; Shimaoka et al. 2002). An irrelevant mouse mAb was used as a negative control. Half of the medium in the hanging drop cultures was carefully removed and substituted with fresh medium containing the corresponding mAb every 12 h to maintain effective concentrations of the antibody. The sequence of the RGD peptide (H-Gly-Arg-Gly-Asp-Thr-Pro-OH) was designed to block a wide spectrum of ECM-binding proteins including collagen, fibronectin, and laminin. The sequence of the RAD peptide was identical with that of the RGD peptide, except that the central Gly residue was substituted with an Ala. Inhibition of E-cadherin activity was achieved by the addition of 5 mM EGTA to remove free extracellular calcium (an essential factor for E-cadherin activation) and by administration of a blocking mAb (clone G10; Santa Cruz Biotechnology) at 10 µg/ml. To restore E-cadherin activity, half of the EGTA-containing medium was removed and replaced with fresh normal growth medium supplemented with 5 mM CaCl<sub>2</sub>.

## Results

### Quantification of shrinkage rates of cell aggregates in spheroid formation

To reveal the dynamics of spheroid formation, we employed a simple method based on the size of cell-projected area as an indicator of compactness of cell aggregates. To test the consistency of the method, the progress of spheroid assembly of two cell lines, each with a distinct capability for adhesion, was tested. Figure 1a

shows the images of HepG2 and Ramos cells taken at 4, 16, 28, and 40 h in hanging drops. HepG2, a cell line of hepatoma origin, was found to pack into a compact spheroid. In contrast, the lymphatic Ramos cells remained loosely bound to each other and failed to show strong cell cohesion. The distinct cell adhesive ability of these two cell types was better illustrated by the difference in their respective shrinkage curves (Fig. 1b). HepG2 showed a continuous increase in compactness with time, displaying a rapid shrinkage rate in the first 12 h, followed by a gradual slowdown, and eventually achieved a steady-stage phase representing the formation of stable spheroid organization after about 36 h of incubation. In contrast, Ramos cells showed only a slight reduction in CI, regardless of the length of incubation time.

To eliminate the variation caused by the differences in cell numbers loaded in each drop, all of the cell-occupied volumes were normalized to that of the same group at the initial 2-h time point. The normalization procedure was verified by loading different numbers of cells per drop, and the changes of the occupied volume were recorded with time. A comparison of the curves before (Fig. 1c) and after (Fig. 1d) normalization revealed that normalization reduced the variation caused by different initial cell numbers to a minimum. Together, these data suggested that the image-based method of compactness measurement provided a quantitative and reproducible way for studying the progression of spheroid assembly.

### Dynamic analysis of spheroid formation in three hepatoma cell lines

Three human hepatoma cell lines, viz., HepG2, Hep3B and PLC/PRF/5, which displayed different phenotypes, were cultured in hanging drops at approximately 500 cells per drop, and the kinetics of cell aggregation was followed. Figure 2 shows the morphology of the aggregates formed by the three types of cell at 24 h of incubation. Even at this early time point, they exhibited a certain degree of difference in compactness. Hep3B cells formed compact spheroids with a smooth surface in which individual cells could not be distinguished. On the other hand, HepG2 cells formed only loose cellular aggregates, and individual cells remained clearly identifiable. No obvious aggregation was observed at 24 h of incubation for PLC/PRF/5 cells, reflecting the poor cohesive activity of the cells. The difference in the cohesive activity of these cells could be clearly illustrated by using the image-based compactness measurement method. As demonstrated in Fig. 2, the compactness of both HepG2 and Hep3B cell aggregates increased rapidly in the first 12 h, and the rate of compaction started to slow down and reached the stationary phase at 36 h for HepG2 and 20 h for Hep3B. The projected area of PLC/PRF/5 cell aggregates was reduced after the first 4 h and continued shrinking but with a much lower rate than those of the other two cell types.

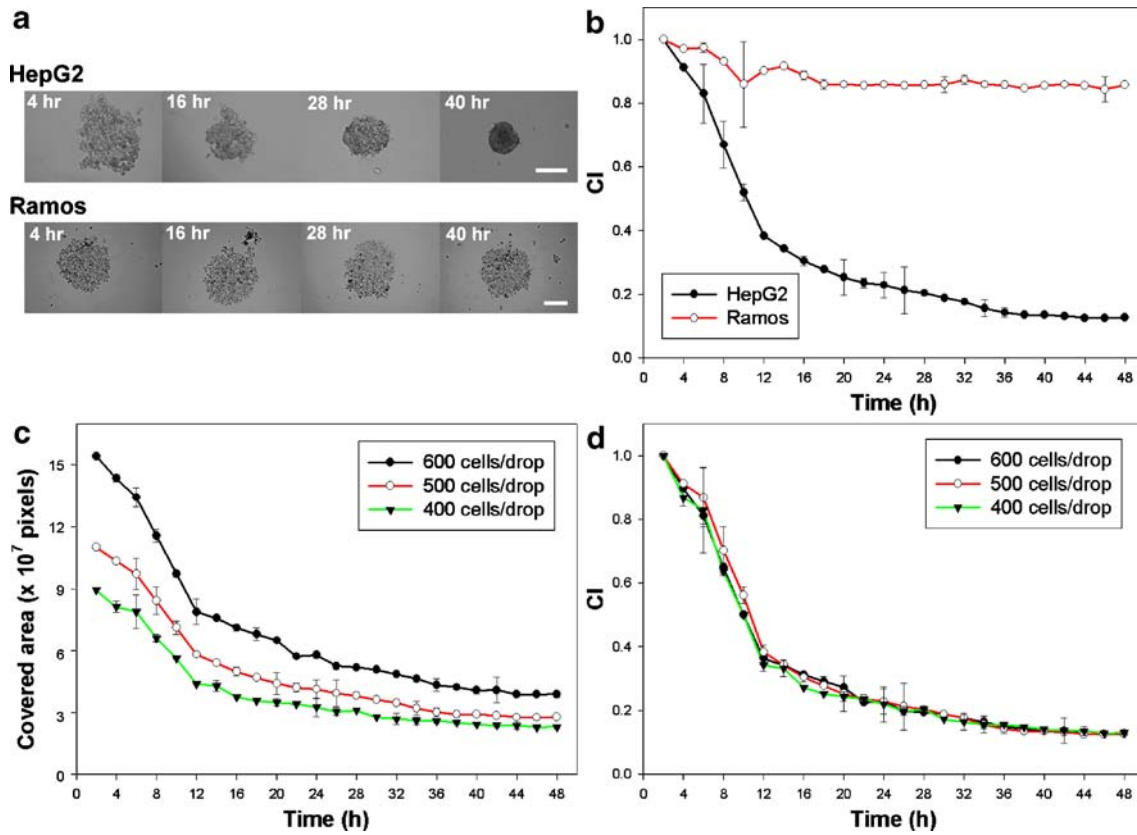


**Fig. 1** Quantitative analysis of spheroid formation. **a** Morphology of HepG2 and Ramos cell aggregates at various time points during spheroid formation. Bar 200  $\mu\text{m}$ . **b** Change of volume of cell aggregates of HepG2 (solid circles) and Ramos cells (open circles)

in hanging drop culture as represented by compactness index (CI). **c, d** The effects of different cell numbers (~400, 500, and 600 HepG2 cells per drop) on the projected area (**c**) and CI (**d**) in hanging drop assays were plotted with time

#### Differential expression of cadherins in hepatoma cell lines

To determine the molecular mechanism responsible for the difference in cell aggregation rates among these hepatoma cell lines, the expression of the genes encoding a known cellular adhesion molecule was analyzed by using real-time PCR. As demonstrated in Table 2, E-cadherin and N-cadherin were the major cadherins expressed in these cells, whereas the expression of P-cadherin and the nonclassical VE-cadherin and LI-cadherin (Wong et al. 2003) could not be detected. Furthermore, Hep3B cells exhibited the highest expression levels of E-cadherin and N-cadherin in comparison with the other two cell lines, implying that the higher expression of these two cadherins is one of the possible reasons that Hep3B cells possess a superior capacity for assembly into spheroids. The low expression levels of E- and N-cadherin in the PLC/PRF/5 line are also consistent with the poor spheroid formation of this cell line.

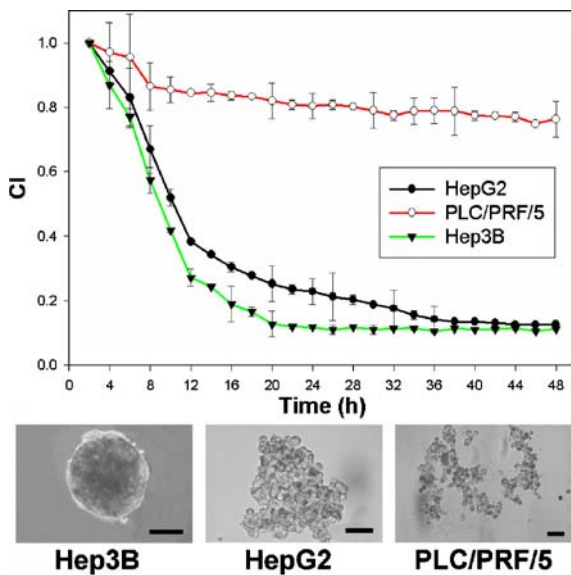


**Fig. 2** Comparative analysis of spheroid-forming capability among three hepatoma cell lines. The CI of the hepatoma cell lines recorded with time during spheroid formation in the hanging drop assay, and the morphology of cell aggregates of Hep3B, HepG2, and PLC/PRF/5 formed in the hanging drop cultured for 24 h. Bar 200  $\mu\text{m}$

#### Secretion of ECM by hepatoma cells

The expression of integrins, which are a set of cell surface proteins that mediate adhesion of cells onto ECM, was investigated. High expression levels of  $\beta 1$ -integrin could

be detected in all the hepatoma cells tested in this study (Table 2). On the other hand, conditioned media collected from Hep3B and HepG2, but not PLC/PRF/5 cells, provided sufficient ECM proteins to assist cell adhesion (Fig. 3), indicating that HepG2 and Hep3B cells synthesized more ECM than can PLC/PRF/5 cells. Thus, in addition to E-cadherin, difference in ECM secretion and subsequent integrin-ECM interaction may be factors that affect hepatoma spheroid formation.

### Effects of ECM on spheroid formation

As the amount of ECM secretion seemed to correlate well with spheroid forming activity in these hepatoma cells, we tested whether the addition of ECM proteins to the culture medium could promote cell aggregation. Single-cell suspensions of HepG2 and PLC/PRF/5 cells were prepared and allowed to grow in hanging drops supplemented with the type I collagen at a concentration ranging from 1 to 30  $\mu\text{g/ml}$ . Significant promotion of aggregation of PLC/PRF/5 cells in a collagen dose-dependent manner was observed as indicated by a left-shift of the shrinkage curve (Fig. 4b). The result strongly suggested that the major reason for the low cohesion in PLC/PRF/5 cells was their low ECM secretion. The promotion effect was less evident in HepG2 cells (Fig. 4a), presumably because a large amount of ECM was synthesized by HepG2 cells. High concentrations ( $>20 \mu\text{g/ml}$ ) of collagen sometimes even disrupted HepG2 spheroid assembly in that the cells formed only small scattered aggregates, and occasionally, cells on the surface migrated out from the small aggregates and formed elongated structures. The spheroid-promotion effects of collagen seemed to require the presence of long-chain fibers because the addition of gelatin, the hydrolytic product of collagen, failed to promote spheroid formation (Fig. 4a,b). In addition, another RGD-motif-containing ECM molecule, fibronectin, also showed the ability to promote HepG2 and PLC/PRF/5 spheroid formation. Collectively, these results strongly suggested that optimal concentrations of long-chain ECM fibers were required for the promotion of spheroid formation.

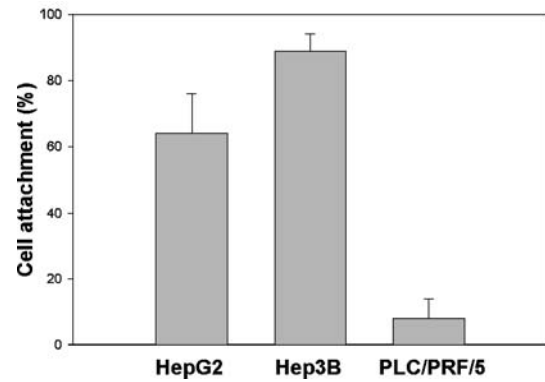


**Fig. 3** Expression of gene encoding cell adhesion molecules in hepatoma cells. The amount of ECM secreted by each of the hepatoma cell lines was determined by functional adherent assays with fluorescent-dye-labeled cells. Comparison of fluorescence counting of cells before and after rinses with PBS yielded the percentage of cell attachment

### Three distinct stages of spheroid formation in PLC/PRF/5 and HepG2 cells

Addition of collagen at a concentration 10  $\mu\text{g/ml}$  altered the aggregate shrinkage curves of HepG2 and PLC/PRF/5 cells and resulted in a three-stage decline, viz., a rapid decrease in size followed by a steady delay period and then another decline (Fig. 4a,b). The delay period lasted about 2–4 h, and during this interval, the CI was kept constant at about 0.32–0.23. The morphology of cells at the delay period resembled the traditional definition of cellular aggregates, in which the boundary of each cell remained distinct. The three-stage kinetics of spheroid formation could be more clearly illustrated by shrinkage rate ( $\Delta\text{CI}/\Delta t$ ) diagrams (Fig. 4c), in which the first peak represented the first stage of rapid shrinking from single-cell suspensions to loose aggregates. After this stage, a delay interval was followed by a smaller peak, which reflected an increase of the rate of cell aggregate compaction. In both HepG2 and PLC/PRF/5, addition of higher concentration of collagen to the culture medium resulted in a further left-shift of the delay period and of the second peak, reflecting faster aggregation (Fig. 4c).

**Table 2** Relative expression of cadherin-encoding genes in the studied hepatoma cells (NA not found)

Gene	HepG2			Hep3B			PLC/PRF/5		
	$C_T$	$dC_T^a$	Folds of activation	$C_T$	$dC_T$	Folds of activation	$C_T$	$dC_T$	Folds of activation
E-cadherin	21.01±0.21	-2.80±0.32	4.11±0.54	20.13±0.19	-1.75±0.26	8.49±0.43	23.14±0.26	-4.83±0.35	1 <sup>b</sup>
N-cadherin	20.21±0.19	-2.00±0.23	13.83±0.43	18.92±0.43	-0.55±0.57	30.06±0.94	24.13±0.32	-5.81±0.43	1
P-cadherin	>40	NA	NA	>40	NA	NA	>40	NA	NA
VE-cadherin	>40	NA	NA	>40	NA	NA	>40	NA	NA
LI-cadherin	>40	NA	NA	>40	NA	NA	>40	NA	NA
$\beta 1$ -integrin	18.02±0.23	0.20±0.32	1.23±0.36	18.21±0.14	-0.16±0.25	0.96±0.27	18.21±0.23	-0.01±0.29	1

<sup>a</sup> $C_T$  value of each gene was normalized by using that of  $\beta$ -actin and was expressed as  $dC_T (= C_{T(\beta\text{-actin})} - C_{T(\text{test})})$

<sup>b</sup>Folds of activation of each gene was calculated by taking the expression levels in PLC/PRF/5 as 1

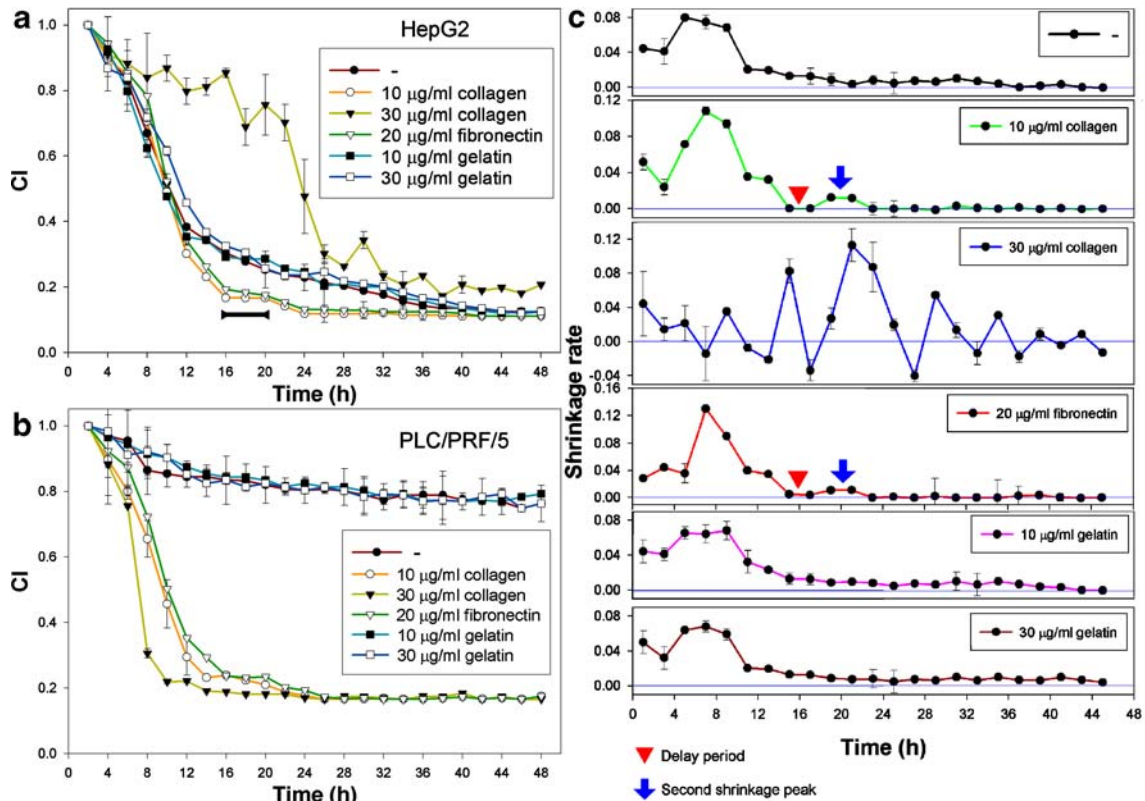


**Fig. 4** Effects of exogenously added collagen, fibronectin, or gelatin on hepatoma spheroid formation. The CI of HepG2 (**a**) and PLC/PRF/5 (**b**) grown in the absence or presence of 10 or 30 µg/ml collagen, 20 µg/ml fibronectin, or 10 or 30 µg/ml gelatin, respectively, was recorded with time. The dynamic profiles of the

shrinkage rate of HepG2 (**c**) during spheroid formation were converted from **a** (arrow second peak of rapid compaction, arrowhead start of delay period). The delay period in **a** is also highlighted

#### Permeability and morphology of cell aggregates at different spheroid assembly stages

As compaction of HepG2 cell aggregates seemed to be a three-stage process, we used permeability to small-molecular-weight fluorescent dye DiI as an indicator to reflect the compactness of the cell aggregates at the different stages. We found that the dye rapidly entered the core of the cell aggregates formed before the delay period (Fig. 5a) and stained the cell membrane red. In contrast, the cell aggregates collected from the stage after the delay period were relatively resistant to penetration of the fluorescent dye and only the cells on the surface of the aggregate could be stained (Fig. 5b). Unlike cell aggregates collected before the delay period, the outer layer of the compact cell aggregates differentiated into smooth, tightly packed, polarized cells (Fig. 5d), consistent with a previous finding that epithelial cells undergo specific differentiation when grown into spheroids (O'Brien et al. 2002). The differentiated surface acted as a physical barrier preventing small molecules such as a fluorescent dye from penetrating the inner parts of spheroids (Fig. 5b).

#### Participation of integrins and ECM in rapid cell aggregation

We further examined the hypothesis that integrins-ECM interaction mediated the rapid assembly of single cells into aggregates by adding 1 mM  $Mg^{2+}$ , in addition to 10 µg/ml collagen, to the hanging drop culture to enhance the activity of integrins (Shimaoka et al. 2002). We used  $Mg^{2+}$ , but not other cations, to avoid cross-activation of cadherin-mediated cell adhesion, which is specifically activated by  $Ca^{2+}$  (Nagar et al. 1996). The combination of  $Mg^{2+}$  and collagen resulted in a strong promotion effect on cell aggregation (Fig. 6). Similar to the action exerted by collagen,  $Mg^{2+}$  promoted primarily the progression from the single-cell suspension to loose cell aggregates and induced an early appearance of the delay period.

The function of integrin could also be modulated by using integrin-specific antibodies or RGD-sequence-containing peptides. In the presence of the  $\beta 1$ -integrin-stimulating mAb clone P4G11, cell aggregation was found to be significantly accelerated (Fig. 6). The profile of the CI vs. time curve was similar with the activation

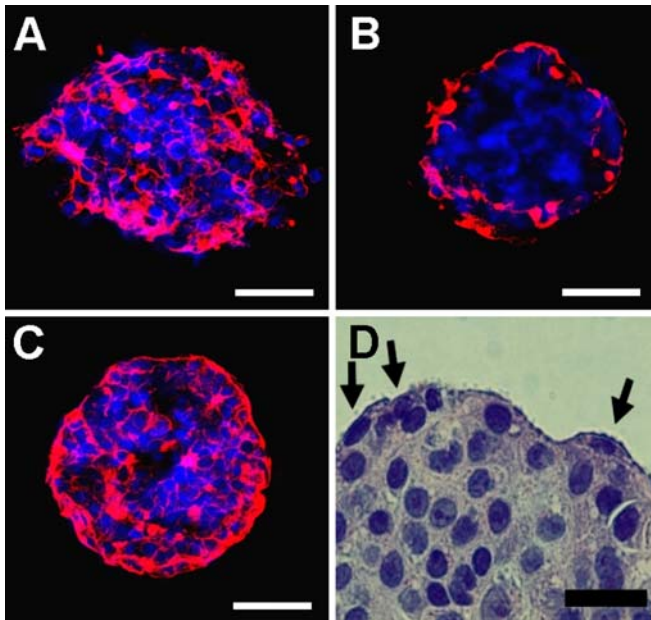


**Fig. 5** Permeability of cell aggregates formed at various stages during spheroid formation. **a, b** Confocal microscopy images of a HepG2 aggregate formed at 16 h (**a**) and 32 h (**b**) in hanging drops. The aggregates were stained with red fluorescent dye DiI and counterstained with Hoechst 33342 (stained nuclei *blue*). **c** HepG2 spheroid completely stained with DiI. *Bar* 50  $\mu\text{m}$ . **d** Hematoxylin and eosin staining of a HepG2 spheroid (*arrows* cells that differentiated to give a smooth epithelium-like surface on the spheroid). *Bar* 20  $\mu\text{m}$

effects triggered by  $\text{Mg}^{2+}$  and high concentrations of collagen, in which the aggregation rates of the first shrinkage stage were enhanced. On the other hand, cell aggregation was strongly inhibited in the presence of clone P5D2 mAb, which is known to block the binding of  $\beta 1$ -integrin to ECM (Fig. 6e). The blocking antibody diminished not only the collagen-mediated promotion effects, but also the appearance of the delay period. Finally, the addition of the RGD peptide, which served as a competitor of ECM-integrin interaction, also resulted in similar inhibition in cell aggregation, whereas no effect was observed with a related but non-functional RAD peptide (Fig. 6). These results demonstrated that cell adhesion onto collagen fibers through the binding of  $\beta 1$ -integrin was essential for the acceleration of cell aggregation.

#### Roles of E-cadherin in the development of compact spheroids from loose aggregates

As the expression of E-cadherin, but not N-cadherin, has been shown to correlate strongly with cell adhesion for the assembly of epithelial tissue (Angres et al. 1996; Islam et al. 1996) and tumor spheroids (Robinson et al. 2003; Shimazui et al. 2004), this cell adhesion molecule was selected for further analysis. The activity of E-cadherin on HepG2 cells was inhibited by using 5 mM EGTA to remove extracellular  $\text{Ca}^{2+}$  or by adding an E-cadherin blocking mAb. The progression of spheroid formation was

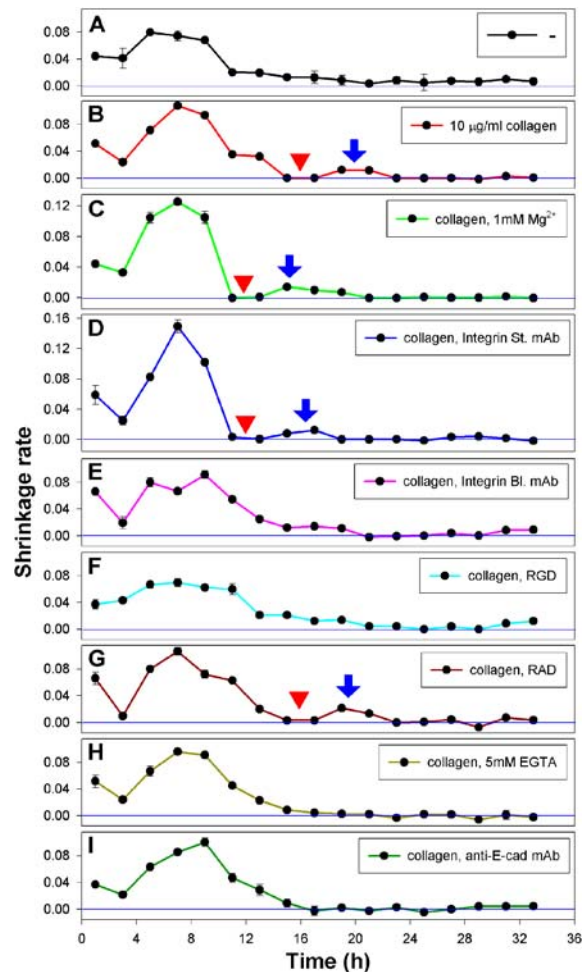


**Fig. 6** Roles of integrin-ECM and E-cadherin interaction on spheroid formation. Comparison of enhancement effects of collagen with or without addition of 1 mM  $\text{Mg}^{2+}$  (**c**), 10  $\mu\text{g}/\text{ml}$  anti- $\beta 1$ -integrin stimulating mAb (**d**) or blocking mAb (**e**), 10  $\mu\text{g}/\text{ml}$  RGD peptide (**f**) or RAD peptide (**g**), 5 mM EGTA (**h**) and 10  $\mu\text{g}/\text{ml}$  anti-E-cadherin blocking mAb (**i**) on HepG2 spheroid formation

examined and, in both cases, cell compaction terminated at the delay period (Fig. 6), corresponding to a loose aggregate morphology, and failed to undergo further compaction to spheroids. Thus, contrary to the promotion of rapid cell aggregation by integrin-ECM in the initial stage of spheroid assembly, cell adhesion mediated by E-cadherin appeared to be essential for the development from loose aggregates to compact spheroids.

#### Participation of integrins in the early stages of spheroid formation

To determine further when integrin was involved in the three stages of spheroid formation, collagen was added at various time points to the hanging drop cultures, and the compactness of the cell aggregates was determined. The addition of 10  $\mu\text{g}/\text{ml}$  collagen at 0, 8, and 16 h caused a rapid shrinkage of the cell aggregates (Fig. 7a). No such effect could be observed if collagen was added after the



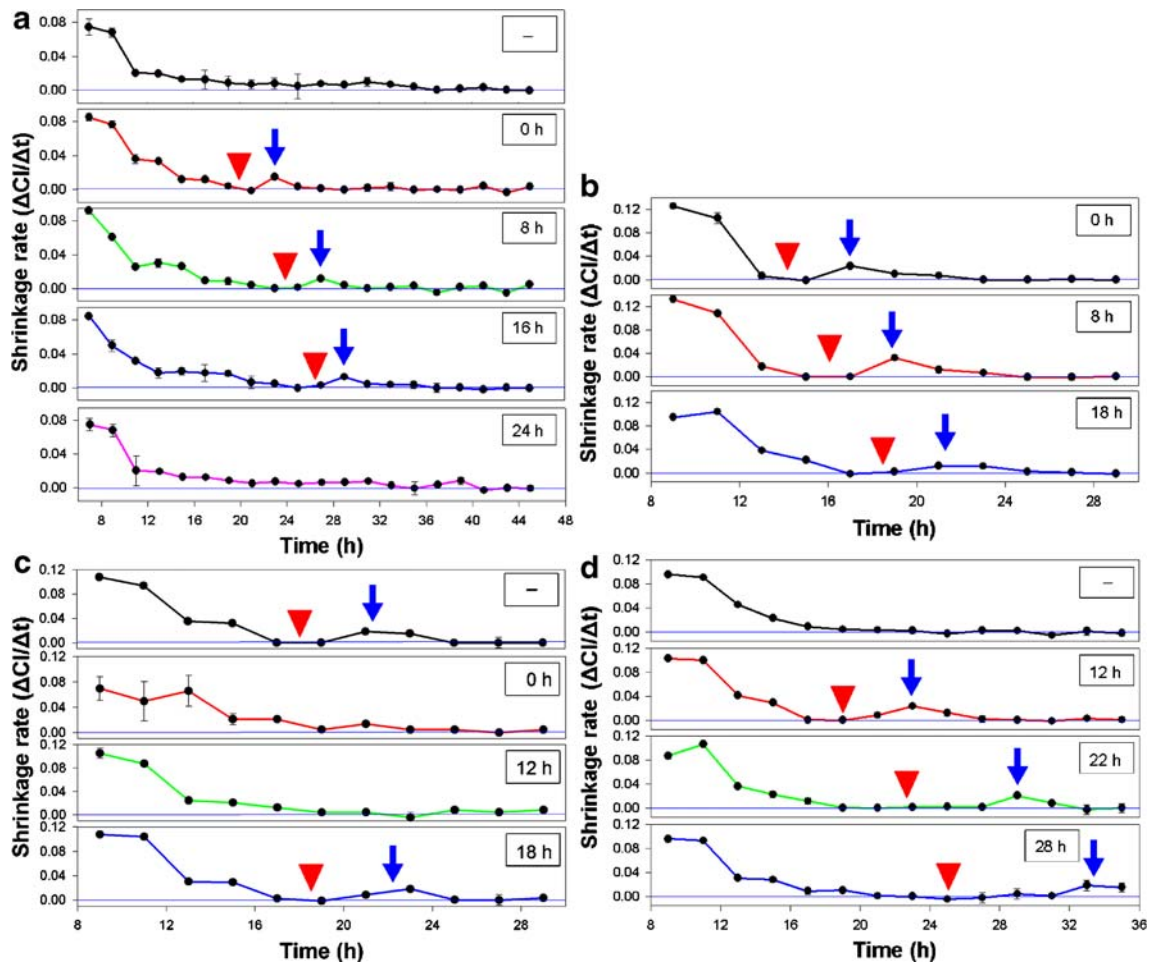


**Fig. 7** Time effects of integrin and E-cadherin action during HepG2 spheroid formation. **a** Determination of the period exhibiting collagen-mediated promoting effects of spheroid formation. Collagen was added before (at 0, 8, and 16 h of incubation) and after (at

24 h of incubation) the delay period. Effects of addition of  $Mg^{2+}$  (**b**), the RGD peptide (**c**), and replenishment of  $Ca^{2+}$  after EGTA treatment (**d**) at various time points

delay period (24 h). Similarly, activation of integrin-ECM interaction with 1 mM  $Mg^{2+}$  (Fig. 7b) or inhibition with the 10  $\mu$ g/ml RGD peptide (Fig. 7c) affected only the cell aggregation rates before the delay period. Thus, integrin activity played a major role in the first stage of cell aggregation.

E-cadherin is required for the compact assembly stage of spheroid formation

Using a similar approach, we attempted to identify the stage at which E-cadherin acted during spheroid formation by treating the cells with EGTA at the start of the hanging drop culture period and by subsequently re-establishing E-cadherin activity at various time points by replenishing  $Ca^{2+}$  exogenously. As shown earlier (Fig. 6), the addition of 5 mM EGTA in the hanging drop culture could block the step from loose aggregates to the formation of compact spheroids. Supplementation of 5 mM  $Ca^{2+}$  to cultures in which the cell aggregation terminated at the delay period re-initiated the shrinkage process (Fig. 7d). The data

suggested that E-cadherin was a dominant factor responsible for establishing strong cohesion and morphological changes.

Expression of E-cadherin gene during spheroid formation

In view of the critical role of E-cadherin in promoting the loose cell aggregates to form compact spheroids, we further examined whether the expression of E-cadherin gene was up-regulated during spheroid formation. A real-time PCR experiment was carried out to monitor the E-cadherin expression level every 8 h during HepG2 spheroid formation. As shown in Fig. 8, at high cell density ( $5 \times 10^5$  cells/ml), which is sufficient to form a spheroid, a gradual increase in E-cadherin expression was noted as spheroid formation progressed. The compact HepG2 spheroid (at 48 h) exhibited a six-fold increase in E-cadherin expression above that of monolayer cells. The  $C_T$  ( $\beta$ -actin) values of all tested samples were found to be consistently in the range of 18.098 to 18.204, whereas the

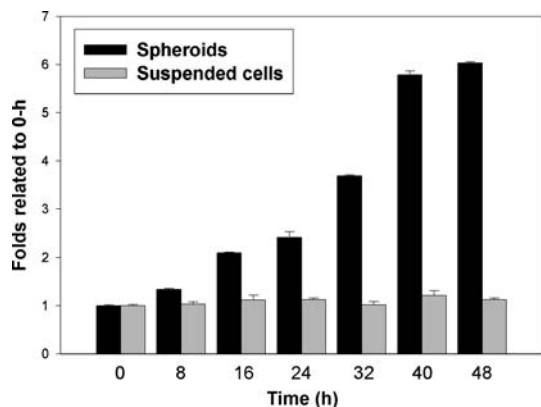


**Fig. 8** Effects of collagen on E-cadherin gene expression. Real-time PCR was performed to demonstrate the change in E-cadherin gene expression during spheroid formation or in scattered cells in medium supplemented with 10  $\mu\text{g/ml}$  collagen

$C_{T(\text{E-cadherin})}$  values gradually decreased from 21.314 (0 h) to 18.780 (48 h). However, at a low cell density ( $5 \times 10^4$  cells/ml), which is too dilute for spheroid formation, no increase in E-cadherin gene expression was observed, even though the same concentration of collagen was added to the culture.

#### Model of spheroid formation

Based on these findings, spheroid formation can be differentiated into a three-stage process, contrary to the seemingly linear aggregation rates. In the initial stage, single cells in suspension are assembled into loose cell aggregates. The long-chain ECM fibers with multiple RGD-containing binding sites for cell-surface integrins provide long-range and rapid aggregation of dispersed cells. After the preliminary aggregation, E-cadherin in turn plays a major role in augmenting cell cohesion by conferring strong cell adhesion through homophilic cadherin-cadherin binding between two adjacent cells. Signal transductions might be initiated through the  $\beta$ -catenin complex (Cavallaro and Christofori 2004) and eventually lead to the exhibition of certain differential characteristics observed in spheroids, such as the smooth interweaved surface as shown in Fig. 5d. Overall, our observations are consistent with the findings of tissue morphogenesis *in vivo*, in which weak integrin-ECM interaction confers the primary binding of cells and later is augmented by stronger cell-cell adhesions as has been detected in tissues *in situ* (Larue et al. 1996).

#### Discussion

In comparison with other techniques for measuring the compactness of cell aggregates, the image-based analysis employed in this study offers advantages of simplicity and reproducibility. By calculating data from a large number of spheroids, the variations caused by a few spheroids with a less than perfect spherical shape can be overcome. The

method is particularly suitable for studying the dynamics of spheroid formation because of its non-disruptive nature and because the size of a single spheroid can be controlled throughout the process.

Several reports have described the use of mathematical models to explain the growth of spheroids and the diffusion of small molecules into cell aggregates. Enmon et al. (2001) have established a kinetic model of spheroid self-assembly from DU-145 prostate cancer cells by using Smoluchowski-like rate equations to analyze the distributions of area projection from random cell aggregates formed in a liquid-overlay culture. Our study has employed a similar image-based dynamic analysis of spheroid assembly but emphasizes more the identification of molecular interactions contributing to spheroid self-assembly. The use of a constant cell number and medium volume in the hanging drops allows us to perform functional manipulation of the cell adhesion molecules easily and accurately, and the stages in which each of these molecules are involved can be clearly defined. We believe that our study is the first to reveal the order, cooperation, and dynamics of these molecules systematically in rebuilding three-dimensional cellular structures.

One question that remains to be elucidated is why there is a delay period. During this period, cells are organized as loose aggregates with high permeability and are mostly spherical in shape. The CI of the aggregates remains steady as if the cells were waiting for a signal to enter the stage of tight compaction. Our real-time PCR analysis has shown an increase in E-cadherin expression during spheroid formation (Fig. 8). Thus, one possible explanation for the presence of the delay period is that the amount of E-cadherin in isolated single cells is not sufficient to allow strong cell-cell interactions. The closer contact between cells in the initial stage, as facilitated by the integrin-ECM interaction, may trigger the expression of E-cadherin. The interaction between E-cadherin molecules is also known to autoregulate E-cadherin gene expression through mitogen-activated protein kinase signaling pathways (Conacci-Sorrell et al. 2003). The delay period is probably the stage for establishing a specific E-cadherin density on the cell surface by *de novo* synthesis; this specific threshold of E-cadherin may drive further cell compaction efficiently. Nevertheless, this hypothesis remains to be verified.

Another question concerns the role of ECM in hepatoma spheroid formation. In this study, ECM molecules are considered as physical linkers to facilitate the convergence of cells. Long-chain collagen or polymerized fibronectin matrix may participate in this process. In addition, from real-time PCR analysis, no increase in E-cadherin gene expression can be observed in low-density cell suspension culture (Fig. 8). No direct promotion of E-cadherin expression seems to occur when collagen is added. ECM binding to  $\beta 1$  and  $\beta 3$  integrins is also known to trigger integrin-linked kinase (ILK) activity; one of the outcomes of this activation is the down-regulation of E-cadherin gene expression (Arusha et al. 2004). Based on this evidence, the promotion of spheroid formation by ECM may arise from physical effects and may not involve cellular signaling.

The study of cell adhesion in spheroid formation can provide important information with respect to tumor metastasis. Multicellular aggregates of ovarian carcinoma cells with sizes ranging from 50 to 750  $\mu\text{m}$  in diameter are sometimes observed in ascitic fluid obtained from patients (Casey et al. 2001). Similarly, metastatic cells of breast cancers and prostate carcinomas form multicellular aggregates intravascularly and attached to the endothelium when being transported by the circulation (Glinsky et al. 2003; Wong et al. 2002). The establishment of cell-cell and cell-ECM interactions in the aggregates is essential to provide survival signals for the circulating cells, preventing them from entering apoptosis because of loss of anchorage (Frisch and Ruoslahti 1997; Frisch and Sreaton 2001; Hanahan and Weinberg 2000). On the other hand, many other tumor cells seem to lose cell cohesion activity and fail to form compact spheroids during the progression of tumor malignancy; this is of especial importance in cancer therapy (Frixen et al. 1991). In such cases, PLC/PRF/5 cells might serve as an excellent model.

Spheroids have been widely used in tissue engineering, bioartificial livers, and embryoid body formation in stem cell research as they have been shown to improve the viability, function, and tissue-specific gene expression of several cultured primary cells (Abu-Absi et al. 2002; Fukuda et al. 2004; Kale et al. 2000; Kelm and Fussenegger 2004; Korff and Augustin 1998; Landry et al. 1985; Lazar et al. 1995; Narayanan et al. 2002; O'Brien et al. 2002). All these applications demand reliable culture conditions for the efficient production of large quantities of spheroids with a uniform size, high cell viability, and proper cell-cell organization. The experimental approaches and the proposed model described in this study should enable optimal conditions for the generation of good quality of spheroids by modulating cadherin and integrin activity, and ECM composition in the cultures. In conclusion, we believe that, with the trend of shifting culture systems from two-dimensional monolayer cells to three-dimensional organoid systems, our dynamic cell aggregation model will be an important reference for those who study spheroids.

## References

- Abu-Absi SF, Friend JR, Hansen LK, Hu WS (2002) Structural polarity and functional bile canaliculi in rat hepatocyte spheroids. *Exp Cell Res* 274:56–67
- Alpaugh ML, Tomlinson JS, Ye Y, Barsky SH (2002) Relationship of sialyl-Lewis(x/a) underexpression and E-cadherin overexpression in the lymphovascular embolus of inflammatory breast carcinoma. *Am J Pathol* 161:619–628
- Angres B, Barth A, Nelson WJ (1996) Mechanism for transition from initial to stable cell-cell adhesion: kinetic analysis of E-cadherin-mediated adhesion using a quantitative adhesion assay. *J Cell Biol* 134:549–557
- Angst BD, Marcozzi C, Magee AI (2001) The cadherin superfamily: diversity in form and function. *J Cell Sci* 114:629–641
- Arusha O, Timothy M, Shoukat D (2004) Regulation of E-cadherin expression and  $\beta$ -catenin/Tcf transcriptional activity by the integrin-linked kinase. *Biochem Biophys Acta* 1691:1–15
- Bates RC, Edwards NS, Yates JD (2000) Spheroids and cell survival. *Crit Rev Oncol Hematol* 36:61–74
- Byers SW, Sommers CL, Hoxter B, Mercurio AM, Tozeren A (1995) Role of E-cadherin in the response of tumor cell aggregates to lymphatic, venous and arterial flow: measurement of cell-cell adhesion strength. *J Cell Sci* 108:2053–2064
- Casey RC, Burleson KM, Skubitz KM, Pambuccian SE, Oegema TR Jr, Ruff LE, Skubitz AP (2001) Beta 1-integrins regulate the formation and adhesion of ovarian carcinoma multicellular spheroids. *Am J Pathol* 159:2071–2080
- Cavallaro U, Christofori G (2004) Cell adhesion and signalling by cadherins and Ig-CAMs in cancer. *Nat Rev Cancer* 4:118–132
- Conacci-Sorrell M, Simcha I, Ben-Yedidia T, Blechman J, Savagner P, Ben-Ze'ev A (2003) Autoregulation of E-cadherin expression by cadherin-cadherin interactions: the roles of beta-catenin signaling, Slug, and MAPK. *J Cell Biol* 163:847–857
- Desoize B (2000) Contribution of three-dimensional culture to cancer research. *Crit Rev Oncol Hematol* 36:59–60
- Enmon RM Jr, O'Connor KC, Lacks DJ, Schwartz DK, Dotson RS (2001) Dynamics of spheroid self-assembly in liquid-overlay culture of DU 145 human prostate cancer cells. *Biotechnol Bioeng* 72:579–591
- Enmon RM Jr, O'Connor KC, Song H, Lacks DJ, Schwartz DK (2002) Aggregation kinetics of well and poorly differentiated human prostate cancer cells. *Biotechnol Bioeng* 80:580–588
- Frisch SM, Ruoslahti E (1997) Integrins and anoikis. *Curr Opin Cell Biol* 9:701–706
- Frisch SM, Sreaton RA (2001) Anoikis mechanisms. *Curr Opin Cell Biol* 13:555–562
- Frixen UH, Behrens J, Sachs M, Eberle G, Voss B, Warda A, Lochner D, Birchmeier W (1991) E-cadherin-mediated cell-cell adhesion prevents invasiveness of human carcinoma cells. *J Cell Biol* 113:173–185
- Fukuda J, Mizumoto H, Nakazawa K, Kajiwara T, Funatsu K (2004) Hepatocyte organoid culture in elliptic hollow fibers to develop a hybrid artificial liver. *Int J Artif Organs* 27:1091–1099
- Glinsky VV, Glinsky GV, Glinskii OV, Huxley VH, Turk JR, Mossine VV, Deutscher SL, Pienta KJ, Quinn TP (2003) Intravascular metastatic cancer cell homotypic aggregation at the sites of primary attachment to the endothelium. *Cancer Res* 63:3805–3811
- Guo W, Giancotti FG (2004) Integrin signalling during tumour progression. *Nat Rev Mol Cell Biol* 5:816–826
- Hanahan D, Weinberg RA (2000) The hallmarks of cancer. *Cell* 100:57–70
- Holtfreter J (1944) A study of the mechanics of gastrulation. *J Exp Zool* 95:171–212
- Islam S, Carey TE, Wolf GT, Wheelock MJ, Johnson KR (1996) Expression of N-cadherin by human squamous carcinoma cells induces a scattered fibroblastic phenotype with disrupted cell-cell adhesion. *J Cell Biol* 135:1643–1654
- Jakab K, Neagu A, Mironov V, Markwald RR, Forgacs G (2004) Engineering biological structures of prescribed shape using self-assembling multicellular systems. *Proc Natl Acad Sci USA* 101:2864–2869
- Kale S, Biermann S, Edwards C, Tarnowski C, Morris M, Long MW (2000) Three-dimensional cellular development is essential for ex vivo formation of human bone. *Nat Biotechnol* 18:954–958
- Kelm JM, Fussenegger M (2004) Microscale tissue engineering using gravity-enforced cell assembly. *Trends Biotechnol* 22:195–202
- Kelm JM, Timmins NE, Brown CJ, Fussenegger M, Nielsen LK (2003) Method for generation of homogeneous multicellular tumor spheroids applicable to a wide variety of cell types. *Biotechnol Bioeng* 83:173–180
- Korff T, Augustin HG (1998) Integration of endothelial cells in multicellular spheroids prevents apoptosis and induces differentiation. *J Cell Biol* 143:1341–1352
- Kunz-Schughart LA, Kreutz M, Knuechel R (1998) Multicellular spheroids: a three-dimensional in vitro culture system to study tumour biology. *Int J Exp Pathol* 79:1–23

- Landry J, Bernier D, Ouellet C, Goyette R, Marceau N (1985) Spheroidal aggregate culture of rat liver cells: histotypic reorganization, biomatrix deposition, and maintenance of functional activities. *J Cell Biol* 101:914–923
- Larue L, Antos C, Butz S, Huber O, Delmas V, Dominis M, Kemler R (1996) A role for cadherins in tissue formation. *Development* 122:3185–3194
- Lazar A, Peshwa MV, Wu FJ, Chi CM, Cerra FB, Hu WS (1995) Formation of porcine hepatocyte spheroids for use in a bioartificial liver. *Cell Transplant* 4:259–268
- Marrs JA, Andersson-Fisone C, Jeong MC, Cohen-Gould L, Zurzolo C, Nabi IR, Rodriguez-Boulan E, Nelson WJ (1995) Plasticity in epithelial cell phenotype: modulation by expression of different cadherin cell adhesion molecules. *J Cell Biol* 129:507–519
- Moscona A, Moscona H (1952) The dissociation and aggregation of cells from organ rudiments of the early chick embryo. *J Anat* 86:287–301
- Mueller-Klieser W (1997) Three-dimensional cell cultures: from molecular mechanisms to clinical applications. *Am J Physiol* 273:C1109–C1123
- Nagar B, Overduin M, Ikura M, Rini JM (1996) Structural basis of calcium-induced E-cadherin rigidification and dimerization. *Nature* 380:360–364
- Nakamura M, Shinji T, Ujike K, Hirasaki S, Koide N, Tsuji T (2002) Cytoskeletal inhibitors, anti-adhesion molecule antibodies, and lectins inhibit hepatocyte spheroid formation. *Acta Med Okayama* 56:43–50
- Narayanan RA, Rink A, Beattie CW, Hu WS (2002) Differential gene expression analysis during porcine hepatocyte spheroid formation. *Mamm Genome* 13:515–523
- Neelamegham S, Munn LL, Zygourakis K (1997) A model for the kinetics of homotypic cellular aggregation under static conditions. *Biophys J* 72:51–64
- O'Brien LE, Zegers MM, Mostov KE (2002) Building epithelial architecture: insights from three-dimensional culture models. *Nat Rev Mol Cell Biol* 3:531–537
- Robinson EE, Zazzali KM, Corbett SA, Foty RA (2003) Alpha5beta1 integrin mediates strong tissue cohesion. *J Cell Sci* 116:377–386
- Robinson EE, Foty RA, Corbett SA (2004) Fibronectin matrix assembly regulates alpha5beta1-mediated cell cohesion. *Mol Biol Cell* 15:973–981
- Shimaoka M, Takagi J, Springer TA (2002) Conformational regulation of integrin structure and function. *Annu Rev Biophys Biomol Struct* 31:485–516
- Shimazui T, Schalken JA, Kawai K, Kawamoto R, Bockhoven A van, Oosterwijk E, Akaza H (2004) Role of complex cadherins in cell-cell adhesion evaluated by spheroid formation in renal cell carcinoma cell lines. *Oncol Rep* 11:357–360
- Tomlinson JS, Alpaugh ML, Barsky SH (2001) An intact overexpressed E-cadherin/alpha,beta-catenin axis characterizes the lymphovascular emboli of inflammatory breast carcinoma. *Cancer Res* 61:5231–5241
- Wong CW, Song C, Grimes MM, Fu W, Dewhirst MW, Muschel RJ, Al-Mehdi AB (2002) Intravascular location of breast cancer cells after spontaneous metastasis to the lung. *Am J Pathol* 161:749–753
- Wong BW, Luk JM, Ng IO, Hu MY, Liu KD, Fan ST (2003) Identification of liver-intestine cadherin in hepatocellular carcinoma—a potential disease marker. *Biochem Biophys Res Commun* 311:618–624